Available online at www.sciencedirect.com
SCIENCE DIRECT®
Tetrahedron 62 (2006) 5510–5518
Tetrahedron

^{1}H and ^{13}C NMR assignments of the three dicyclopenta-fused pyrene congeners

María José Otero-Lobato,[a] Cornelis A. van Walree,[a] Remco W. A. Havenith,[b] Leonardus W. Jenneskens,[a,*] Patrick W. Fowler[c] and Erich Steiner[d]

[a]*Debye Institute, Organic Chemistry and Catalysis, Utrecht University, Padualaan 8, 3584 CH Utrecht, The Netherlands*
[b]*Debye Institute, Theoretical Chemistry Group, Utrecht University, Padualaan 8, 3584 CH Utrecht, The Netherlands*[†]
[c]*Department of Chemistry, University of Sheffield, Sheffield S3 7HF, UK*
[d]*School of Biosciences, University of Exeter, Stocker Road, Exeter EX4 4QD, UK*

Received 25 January 2006; accepted 9 March 2006
Available online 12 April 2006

Abstract—Complete ^{1}H and ^{13}C NMR assignments of the (di-)cyclopenta-fused pyrene congeners, cyclopenta[*cd*]- (**2**), dicyclopenta[*cd*,*fg*]- (**3**), dicyclopenta[*cd*,*jk*]- (**4**) and dicyclopenta[*cd*,*mn*]pyrene (**5**), respectively, are achieved using two-dimensional (2D) NMR spectroscopy. The experimental ^{13}C chemical shift assignments are compared with computed ab initio CTOCD-*PZ2*/6-31G** ^{13}C chemical shifts; a satisfactory agreement is found. Substituent-induced chemical shifts in the pyrene core induced by annelation of cyclopenta moieties are discussed. Effects of dicyclopenta topology on electronic structure are illustrated for **3**–**5**.

1. Introduction

The (di-)cyclopenta-fused congeners of pyrene (**1**), viz. cyclopenta[*cd*]- (**2**),[1] dicyclopenta[*cd*,*fg*]- (**3**), dicyclopenta-[*cd*,*jk*]- (**4**) and dicyclopenta[*cd*,*mn*]pyrene (**5**),[2,3] belong to an important sub-class of the polycyclic aromatic hydrocarbons (PAHs) known as cyclopenta-fused PAHs (CP-PAHs) (Fig. 1).

The independent synthesis of CP-PAHs **2**–**5** has been instrumental for their identification as significant constituents of the nonpolar fraction of combustion exhausts derived from organic matter, viz. fossil fuels.[4–6] Compounds **3**–**5** have also been put forward as undesired side-products that are formed during thermal treatment of pyrene-contaminated soil.[7] Since CP-PAHs like **2**–**5** may exhibit mutagenic and carcinogenic properties,[8] they represent a potential human health concern.[9–15] Only recently the bacterial mutagenicity response of **3**–**5** was assayed employing the standard Ames-assay (*Salmonella typhimurium* strain TA98 with and without exogenous metabolic activation (±S9-mix)). CP-PAHs **3**–**5** were found to be highly active metabolic-dependent mutagens. Interestingly, congeners **3** and **5** were found to act as direct mutagens, that is, they are potent mutagens even in the absence of exogenous metabolic activation.[16]

From a fundamental perspective the nonalternant CP-PAHs **3**–**5** also possess unusual physico-chemical properties, such as high electron affinities (low one-electron reduction potentials),[17–20] characteristic upfield-shifted ^{1}H NMR

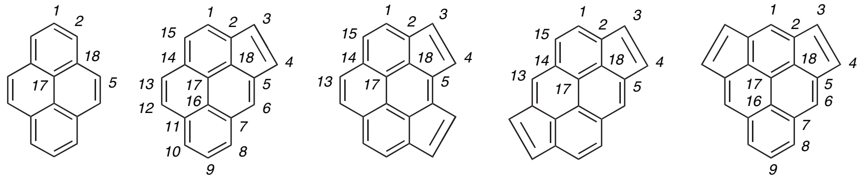

Figure 1. Pyrene (**1**), cyclopenta[*cd*]- (**2**), dicyclopenta[*cd*,*fg*]- (**3**), dicyclopenta[*cd*,*jk*]- (**4**) and dicyclopenta[*cd*,*mn*]pyrene (**5**). A generalized carbon atom numbering scheme is used to facilitate the comparison of related positions in compounds **1**–**5**.

---

* Corresponding author. Tel.: +31 30 2533128; fax: +31 30 2534533; e-mail: l.w.jenneskens@chem.uu.nl
[†] Affiliated to Organic Chemistry and Catalysis.

0040–4020/$ - see front matter © 2006 Elsevier Ltd. All rights reserved.
doi:10.1016/j.tet.2006.03.033

chemical shifts,[2,3,21] and photophysical properties, viz. UV–vis spectra that are strongly modulated by the number and topology of the annelated cyclopenta moieties[2,20] and anomalous fluorescence.[22] As a consequence, CP-PAHs **3**–**5** represent interesting probe molecules in the study of the energy and magnetic criteria of aromaticity in π-conjugated polycyclic systems. For **1**–**5** it has been shown both experimentally and theoretically that the number and topology of the annelated cyclopenta moieties markedly affects the global and local (distinct rings) aromatic character of **1**–**5**.[23–25] In another connection, **3**–**5** have been proposed as potential intermediates in the formation of fullerenes under flame conditions.[5,26–28]

The complete ^{1}H and ^{13}C NMR assignments of **3**–**5**, so far unreported, are the subject of this paper. Although the ^{1}H and ^{13}C NMR assignments of cyclopenta[*cd*]pyrene (**2**, $C_{18}H_{10}$) have been reported previously,[29,30] the assignment of some of its quaternary carbon atoms (C*14* and C*17*, see Fig. 1) remains ambiguous. Hence, **2** is also reinvestigated. Furthermore, a comparison of the experimental ^{13}C assignments with computed ab initio CTOCD-*PZ2*/6-31G** ^{13}C chemical shifts are carried out. Hence, conclusions can be drawn as to the effect of cyclopenta annelation to a pyrene perimeter on the ^{1}H[23,25] and ^{13}C chemical shifts (substituent-induced chemical shifts, SCS; $\Delta\delta$ with **2** as the reference compound for **3**–**5**, respectively) can be drawn.

2. Results and discussion

The ^{1}H and ^{13}C NMR assignments of **2**–**5** were achieved using two-dimensional (2D) NMR techniques. Nuclear Overhauser Effect Spectroscopy (NOESY) was used for the assignment of proton signals by evaluation of *through-space* dipolar interactions. Heteronuclear Chemical Shift Correlation (HETCOR) was applied to identify those carbon atoms bearing hydrogen. Long-Range (LR)-HETCOR reflecting one to three bond C–H couplings ($^1J_{C\text{–}H}$–$^3J_{C\text{–}H}$) was used to make a definitive assignment of the quaternary carbon atoms. Since not all expected $^2J_{C\text{–}H}$ and/or $^3J_{C\text{–}H}$ couplings could be observed in a single LR-HETCOR experiment, different experiments employing different long-range C–H coupling constants (range 4–10 Hz), were executed in order to visualize all the different correlations. In some cases, long-range C–H interactions were still not discernible, presumably because their $^nJ_{C\text{–}H}$ values deviate from the common long-range coupling constants used in LR-HETCOR experiments (4, 6, 8 or 10 Hz). Note that $^3J_{C\text{–}H}$ values normally fall in the range of 4–10 Hz while $^2J_{C\text{–}H}$ and $^4J_{C\text{–}H}$ values are typically less than 4 and 2 Hz, respectively.[31]

2.1. Experimental NMR spectra

2.1.1. Cyclopenta[*cd*]pyrene (2). ^{1}H and ^{13}C NMR assignments of **2** (C_s symmetry) were first reported by Jans et al.[29] However in a more recent study,[30] in which partially ^{13}C-labelled **2** was used, the original assignment of the quaternary carbon atoms C2, C7, C*14*, C*16* and C*17* was questioned (Figs. 1 and 2). This prompted us to also take **2** into consideration. Since all ^{1}H NMR resonances of **2** have been assigned unambiguously (Table 1),[29,30,32] the carbon atoms of this molecule that bear hydrogen were readily identified using HETCOR. The ^{13}C resonances at δ 133.48 and 130.52 show a cross peak with δ 7.47 (H*3*) and 8.38 (H*8*), respectively, and thus originate from C*3* and C*8*, respectively. Following similar reasoning the ^{13}C resonances at δ 128.54, 127.81, 126.94, 126.93, 126.57, 126.48, 124.34 and 122.68 correspond to C*10*, C*4*, C*9*, C*12*, C*13*, C*6*, C*1* and C*15*, respectively, (see Fig. 2). These results are all in line with those previously reported.

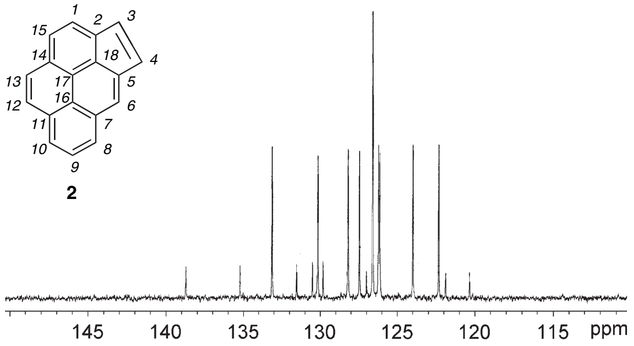

Figure 2. 1D ^{13}C NMR spectrum (solvent $CDCl_3$) of cyclopenta[*cd*]pyrene (**2**, see also Table 1).

Next, various LR-HETCOR experiments, in which different long-range $^nJ_{C\text{–}H}$ coupling constants were used, were performed (Table 1 and see Section 4.1) in order to assign the eight quaternary carbon atoms of **2**. Since with LR-HETCOR two- ($^2J_{C\text{–}H}$) and three-bond ($^3J_{C\text{–}H}$) long-range couplings between quaternary carbon atoms and distant hydrogens are most likely to be observed[33] only these types of contributions are considered. The hydrogens H*6*, H*3* and H*4* (Fig. 1) show a cross peak with the ^{13}C resonance at δ 139.07, which can only correspond to either C*5* or C*18*. The ^{13}C resonance at δ 135.58 shows cross-peaks with H*1* and H*4*, implying that this resonance originates either from C*2* or C*18*. H*3* and H*4* also show a cross peak with the ^{13}C resonance at δ 127.34 , which may then correspond to C*2*, C*5* or C*18*. To distinguish between these three carbon atoms, the proton-decoupled 1D ^{13}C NMR spectrum of **2** (Fig. 2) is carefully examined. The ^{13}C resonance at δ 127.34 possesses the lowest intensity. This suggests that it belongs to a carbon atom located within the pyrene core, viz. C*18*. Owing to its increased distance from the hydrogens of the pyrene perimeter, its relaxation will be slower, leading to a reduced intensity.[34] If the assignment of C*18* (δ 127.34) is correct, it implies that the ^{13}C resonances at δ 139.07 and 135.58 correspond to C*5* and C*2*, respectively. The cross-peaks found between the ^{13}C signal at δ 130.87 and H*12* and H*13*, indicate that this ^{13}C resonance must originate either from C*11* or C*14*. The δ 131.90 signal can correspond only to C*7*, since it exhibits only cross-peaks with H*6* and H*9*. In analogy, the ^{13}C resonance at δ 122.23 shows interactions with H*6*, H*8*, H*10* and H*13*. This means that it can arise only from C*16*. With the identification of C*16*, the ^{13}C resonance at δ 130.18 can be assigned to C*11* due to its cross-peaks with H*10* and H*12*. The available assignments now permit the identification of C*14* at δ 130.87. By elimination, the ^{13}C resonance at δ 120.69 belongs to C*17*. The complete ^{1}H and the ^{13}C assignments of **2** are summarized in Table 1.

2.1.2. Dicyclopenta[*cd*,*fg*]pyrene (3). Since dicyclopenta[*cd*,*fg*]pyrene (**3**, $C_{20}H_{10}$) possesses C_{2v} symmetry, its

Table 1. Cross-peaks observed in the HETCOR and LR-HETCOR spectra of cyclopenta[*cd*]pyrene (**2**)[a,b]

Nucleus	δ (^{13}C) ppm	H*8*	H*6*	H*10*	H*1*	H*15*	H*12*	H*9*	H*13*	H*3*	H*4*
		8.38 (d, $^3J_{H–H}$ 7.70 Hz)	8.36 (s)	8.28 (d, $^3J_{H–H}$ 7.60 Hz)	8.12 (m)	8.08 (m)	8.03 (m)	8.00 (m)	7.98 (m)	7.47 (d, $^3J_{H–H}$ 5.10 Hz)	7.27 (d, $^3J_{H–H}$ 5.10 Hz)
C*17*	**120.69**					b,c,d					
C*16*	**122.23**	a	d	c					c,d		
C*15*	122.68					HT					
C*1*	124.34				HT	b					
C*6*	126.48		HT					c,d			
C*13*	126.57						c		HT		
C*12*	126.93		a				HT				
C*9*	126.94							HT			
C*18*	**127.34**									d	d
C*4*	127.81		a,d								HT
C10	128.54		b	HT				d			
C*11*	**130.18**			b			d				
C*8*	130.52	HT	a,d	c							
C*14*	**130.87**						d		b		
C*7*	**131.90**		a,c					b,d			
C*3*	133.48									HT	a
C*2*	**135.58**				d						c,d
C*5*	**139.07**		a							d	a

[a] See Figure 1 for the structure and atom numbering of **2**. In Figure 2 the experimental 1D ^{13}C NMR spectrum of **2** is shown. Quaternary carbon atoms are typeset in boldface and the multiplicity of the ^{1}H chemical shifts is indicated between parentheses.

[b] HETCOR cross-peaks ($^1J_{C–H}$ coupling constant 160 Hz, H relaxation delay 1 s) are indicated as HT. Independent LR-HETCOR experiments gave the cross-peaks indicated as observed with long-range coupling constants of 4 Hz (a), 6 Hz (b), 8 Hz (c) and 10 Hz (d) (relaxation delay 4 s).

^{1}H and ^{13}C NMR spectrum contains five and ten distinct resonances, respectively, (1D ^{13}C NMR, Fig. 3). In its ^{1}H NMR spectrum, the singlet at δ 7.45 (2H) is readily assigned to hydrogen H*13*. In addition, the vicinal hydrogen pairs H*1* and H*15*, and, H*3* and H*4*, can be distinguished on the basis of their different $^3J_{H–H}$ coupling constants, as the hydrogens of the externally fused cyclopenta-rings (H*3* and H*4*) possess a characteristic $^3J_{H–H}$ coupling constant of ca. 5 Hz. The ^{1}H assignments of **3** are completed by an NOESY experiment. The presence of cross-peaks between the doublet at δ 7.63 (2H, $^3J_{H–H}$ 7.60 Hz) and 7.03 (2H, $^3J_{H–H}$ 5.30 Hz) reveals that the former corresponds to H*1* and the latter to H*3*, respectively. Consequently, the doublets at δ 6.49 (2H, $^3J_{H–H}$ 5.30 Hz) and 7.72 (2H, $^3J_{H–H}$ 7.60 Hz) belong to H*4* and H*15*, respectively.

The unequivocal ^{1}H assignments of **3** now allow the identification of all the carbon atoms bearing hydrogen (HETCOR; see Fig. 4 for an illustrative example). The ^{13}C resonances positioned at δ 137.31, 127.88, 127.07, 127.03 and 123.45 belong to C*3*, C*4*, C*15*, C*13* and C*1*, respectively, (Table 2).

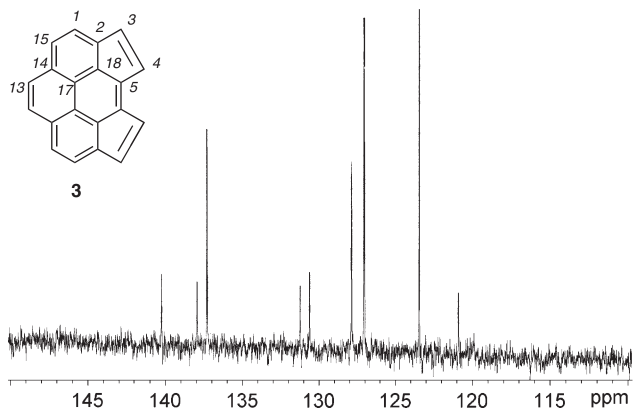

Figure 3. Experimental 1D ^{13}C NMR spectrum of dicyclopenta[*cd*,*fg*]-pyrene (**3**, see also Table 2).

Independent LR-HETCOR experiments optimized for different long-range $^nJ_{C–H}$ coupling constants (Table 2 and see Section 4.1) enabled the assignment of all the quaternary carbon atoms of **3** (see Fig. 4 for an illustrative example). Only $^nJ_{C–H}$ long-range interactions with n=2 or 3 between hydrogens and the quaternary carbon atoms are taken into consideration (vide supra). Hydrogen H*1* shows two cross-peaks with the ^{13}C resonances at δ 130.62 and 131.23, which may then correspond to either C*14* ($^3J_{C–H}$), C*2* or C*18* ($^2J_{C–H}$). Hydrogen H*13* shows two cross-peaks with the ^{13}C resonances at δ 130.62 and 120.91, which may thus arise from C*14* ($^2J_{C–H}$) or C*17* ($^3J_{C–H}$). Since the ^{13}C (δ 130.62) resonance was also found to interact with hydrogen H*1*, it can only correspond to C*14*. Consequently, the δ 120.91 ^{13}C signal belongs to C*17*. Hydrogen H*15* shows cross-peaks at δ 120.91 (C*17*) and 140.24, which may originate from C*2* ($^3J_{C–H}$) and C*14* ($^2J_{C–H}$). Since C*14* (δ 130.62) has already been assigned, the ^{13}C resonance at δ 140.24 has to correspond to C*2*. Thus, the ^{13}C signal at δ 131.23 belongs to C*18*. By elimination, the ^{13}C resonance at δ 137.94 then corresponds to C*5*. This is confirmed by the observation of cross-peaks at δ 137.94 with *H3* ($^3J_{C–H}$) and H*4* ($^2J_{C–H}$). The complete ^{1}H and ^{13}C NMR assignments of **3** are summarized in Table 2.

2.1.3. Dicyclopenta[*cd*,*jk*]pyrene (4).

In the case of dicyclopenta[*cd*,*jk*]pyrene (**4**, $C_{20}H_{10}$), which possesses C_{2h} symmetry, five and ten distinct resonances, respectively, are found in the ^{1}H and ^{13}C NMR spectra (Fig. 5). The total ^{1}H assignment was accomplished by an NOESY experiment. The cross peak between the singlet at δ 7.50 (2H), which corresponds to H*13*, and the doublet at δ 6.62 (2H, $^3J_{H–H}$ 5.21 Hz) indicates that the latter arises from H*4* (cf. the characteristic $^3J_{H–H}$ coupling constant of ca. 5 Hz for the vicinal olefinic hydrogens in the annelated five-membered rings).

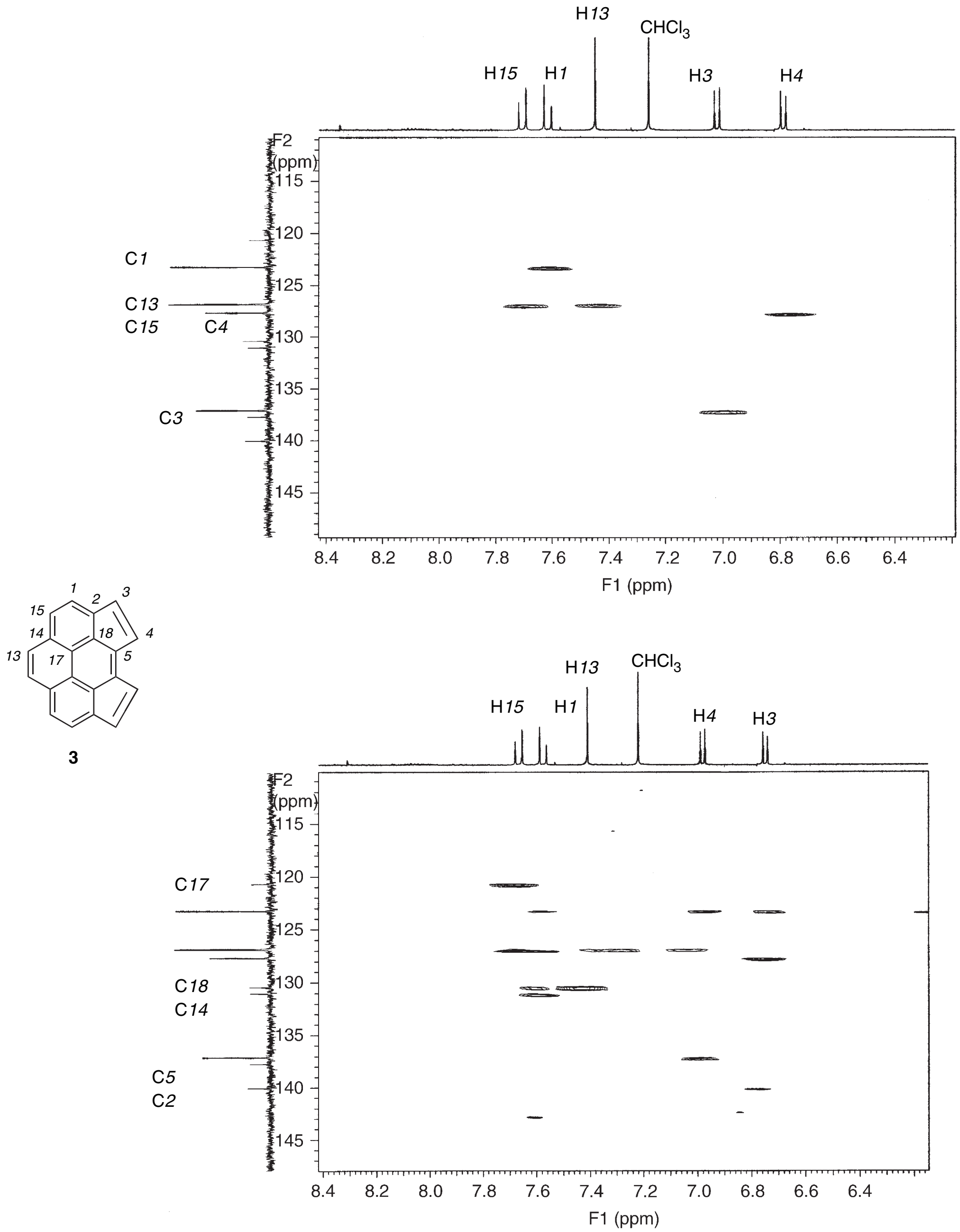

Figure 4. HETCOR ($^1J_{C–C}$ 160 Hz, top) and LR-HETCOR ($^1J_{C–C}$ 160 Hz and $^nJ_{C–H}$ 8 Hz, bottom) spectra of dicyclopenta[*cd*,*fg*]pyrene (**3**).

Another interaction is found between the doublet at δ 7.47 (2H, $^3J_{H–H}$ 7.69 Hz) and the doublet at δ 6.71 (2H, $^3J_{H–H}$ 5.21 Hz). Thus, H*1* corresponds to δ 7.47 and H*3* to 6.71. Since all ^{1}H NMR signals of **4** have been now identified, those of its carbons atoms bearing a hydrogen can be assigned using HETCOR: δ 133.49 corresponds to C*3*, δ131.63 to C*4*, 129.63 to C*15*, 125.72 to C*13* and 122.40 to C*1* (Fig. 4 and Table 3).

The LR-HETCOR experiments with different long-range C–H coupling constants were used (Table 3 and see Section 4.1) in order to assign the quaternary carbon atoms of **4**. Hydrogen H*1* shows two cross-peaks with the ^{13}C resonances at δ 130.66 and 132.07, which can arise from C*14*, C*18* ($^3J_{C–H}$) and C*2* ($^2J_{C–H}$). H*15* exhibits interactions with the ^{13}C resonances at δ 141.00 and 121.44, which may then correspond to C*2* and C*17* ($^3J_{C–H}$) or C*14* ($^2J_{C–H}$). The ^{13}C resonance at δ 141.00 gives another cross peak with H*4*. Thus, we assign δ 141.00 to C*2* ($^3J_{C–H}$), as C*14* and C*17* would present a four- ($^4J_{C–H}$) and a five-bond ($^5J_{C–H}$) coupling with H*4*, respectively, which is unlikely to be observed under the applied experimental conditions.[33] Since the cross-peaks for H*1* with δ 130.66 and 132.07 can now only arise from C*14* and C*18*, this leaves δ 121.44 for C*17*. By elimination, it is now possible to relate ^{13}C signal at δ 140.42 to C*5*. These assignments are supported by the behaviour of H*13*, which exhibits two cross-peaks at δ 121.44 (C*17*), and 130.66, which can arise from the interaction with C*18* ($^3J_{C–H}$) or C*14* ($^2J_{C–H}$). The final assignment for C*14* and C*18* is achieved by comparing their intensities in the 1D ^{13}C NMR spectrum of **4** (Fig. 5). The intensity of the ^{13}C signal at δ 132.07 is stronger than that at δ 130.66. This strongly

Table 2. Cross-peaks observed in the HETCOR and LR-HETCOR spectra of dicyclopenta[*cd*,*fg*]pyrene (**3**)[a,b]

Nucleus	δ (^{13}C) ppm	H*15*	H*1*	H*13*	H*3*	H*4*
		7.72 (d, $^3J_{H-H}$ 7.60 Hz)	7.63 (d, $^3J_{H-H}$ 7.60 Hz)	7.45 (s)	7.03 (d, $^3J_{H-H}$ 5.30 Hz)	6.49 (d, $^3J_{H-H}$ 5.30 Hz)
C*17*	**120.91**	a,b		a		
C*1*	123.45	c	HT		b	a
C*13*	127.03	b	b	HT		
C*15*	127.07	HT		b		
C*4*	127.88				b	HT
C*14*	**130.62**		a,b	a,b,c		
C*18*	**131.23**		a,b,c			
C*3*	137.31				HT	a
C5	**137.94**				c	c
C2	**140.24**	a				b,c

[a] See Figure 1 for the structure and atom numbering of **3**. In Figure 3 the 1D ^{13}C NMR spectrum and in Figure 4 a HETCOR (top) and an LR-HETCOR (bottom) 2D spectra of **3** are shown. Quaternary carbon atoms are typeset in boldface and the multiplicity of the ^{1}H chemical shifts is indicated between parentheses.

[b] HETCOR cross-peaks are indicated as HT. LR-HETCOR experiments gave the cross-peaks shown as observed with long-range coupling constants of 6 Hz (a), 8 Hz (b) and 10 Hz (c).

Table 3. Cross-peaks observed in the HETCOR and LR-HETCOR spectra of dicyclopenta[*cd*,*jk*]pyrene (**4**)[a,b]

Nucleus	δ (^{13}C) ppm	H*15*	H*13*	H*1*	H*3*	H*4*
		7.71 (d, $^3J_{H-H}$ 7.69 Hz)	7.50 (s)	7.47 (d, $^3J_{H-H}$ 7.69 Hz)	6.71 (d, $^3J_{H-H}$ 5.21 Hz)	6.62 (d, $^3J_{H-H}$ 5.21 Hz)
C*17*	**121.44**	b,c,d	b,c			
C*1*	122.40	b,c		HT		
C*13*	125.72	a,b	HT			
C*15*	129.63	HT	a,b,c	c,d		
C*18*	**130.66**		c,d	b		
C*4*	131.63					HT
C14	**132.07**			b,c		
C*3*	133.49		c		HT	a
C5	**140.42**					
C2	**141.00**	a,b				a

[a] See Figure 1 for the structure and atom numbering of **4**. In Figure 5 the 1D ^{13}C NMR spectrum of **4** is shown. Quaternary carbon atoms are typeset in boldface and the multiplicity of the ^{1}H chemical shifts are indicated between parentheses.

[b] HETCOR cross-peaks are indicated as HT. LR-HETCOR experiments gave the cross-peaks shown as observed with long-range coupling constants of 4 Hz (a), 6 Hz (b), 8 Hz (c) and 10 Hz (d).

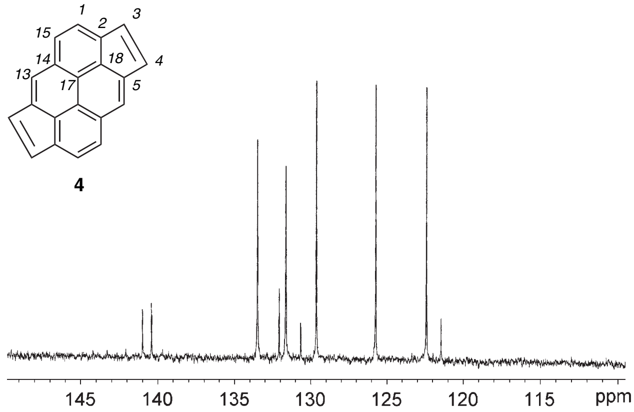

Figure 5. 1D ^{13}C NMR spectrum (solvent $CDCl_3$) of dicyclopenta[*cd*,*jk*]-pyrene (**4**, see also Table 3).

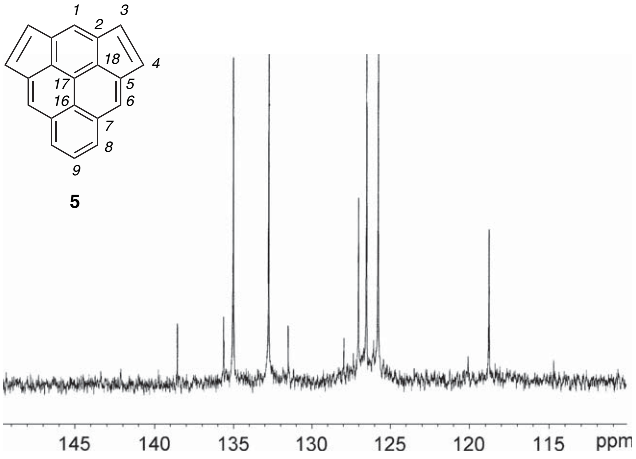

Figure 6. 1D ^{13}C NMR spectrum (solvent $CDCl_3$) of dicyclopenta[*cd*,*mn*]-pyrene (**5**, see also Table 4).

indicates that the ^{13}C resonances at δ 132.07 and 130.66 must originate from C*14* and from C*18*, respectively, since the latter carbon atom is more distant from the hydrogen containing pyrene perimeter.[34] The complete ^{1}H and ^{13}C NMR assignments of **4** are compiled in Table 3.

2.1.4. Dicyclopenta[*cd*,*mn*]pyrene (5).

Dicyclopenta[*cd*,*mn*]pyrene (**5**, $C_{20}H_{10}$) possesses C_{2v} symmetry. This may give six and twelve distinct signals in the ^{1}H and ^{13}C NMR spectra (Fig. 6). Several of the ^{1}H resonances of **5** are readily assigned. The triplet at δ 8.08 (1H, $^3J_{H-H}$ 7.70 Hz) has to correspond to hydrogen H*9*. The singlets at δ 8.15 (1H) and 8.37 (2H) have to originate from H*1* and H*6*, respectively, and the doublet at δ 8.53 (2H, $^3J_{H-H}$ 7.70 Hz) belongs to H*8*. The doublets at δ 7.51 (2H, $^3J_{H-H}$ 5.10 Hz) and 7.26 (2H, $^3J_{H-H}$ 5.10 Hz) corresponds to H*3* and H*4* or vice versa (cf. the characteristic $^3J_{H-H}$ value of ca. 5 Hz for an olefinic hydrogens in a five-membered ring). An NOESY spectrum reveals cross-peaks between the singlet at δ 8.37 (H*6*) and the doublet at δ 7.26, on one hand, and the singlet at δ 8.15 (H*1*) and the doublet at δ 7.51, on the other hand. Thus, the doublets at δ 7.51 and 7.26 originate from H*3* and H*4*. As the complete ^{1}H NMR assignments of **5** have been achieved, its carbon atoms bearing hydrogen were identified using HETCOR (Table 2). The results show that the ^{13}C resonances located at δ 135.03, 132.76, 127.04, 126.53, 125.80 and 118.78 correspond to C*3*, C*8*, C*9*, C*4*, C*6* and C*1*, respectively.

The LR-HETCOR experiments with different long-range $^nJ_{C-H}$ coupling constants allow the assignments of the quaternary C atoms of **5** (Table 4 and see Section 4.1). For H*9* two cross-peaks are observed with the ^{13}C resonances at δ 120.10 and 127.96, which may correspond to C*7* and C*16*. Note, however, that for *C16* the interaction with H*9* has to be a long-range $^4J_{C-H}$ coupling. Hydrogen H*6* correlates with the ^{13}C signals positioned at δ 127.96, 131.52 and 138.56; possible assignments for these cross-peaks are C*7* and C*5* ($^2J_{C-H}$) or C*18* and C*16* ($^3J_{C-H}$). The ^{13}C resonances at δ 131.52 and 138.56 can only correspond to C*5* and C*18*, since the ^{13}C signal at δ 127.96 already has been assigned to either C*7* or C*16*. H*3* correlates with both the δ 131.52 and

Table 4. Cross-peaks observed in the HETCOR and LR-HETCOR spectra of dicyclopenta[*cd*,*mn*]pyrene (**5**)[a,b]

Nucleus	^{13}C (ppm)	H*8*	H*6*	H*1*	H*9*	H*3*	H*4*
		8.53 (d, $^3J_{H-H}$ 7.70 Hz)	8.37 (s)	8.15 (s)	8.08 (t, $^3J_{H-H}$ 7.70 Hz)	7.51 (d, $^3J_{H-H}$ 5.10 Hz)	7.26 (d, $^3J_{H-H}$ 5.10 Hz)
C17	**114.71**						
C*1*	118.78			HT			
C16	**120.10**				b		
C*6*	125.80	b	HT				
C*4*	126.53						HT
C*9*	127.04		a		HT		
C7	**127.96**		c		b		
C18	**131.52**		a			a	a
C*8*	132.76	HT	b				
C*3*	135.03					HT	c
C2	**135.63**					b	c
C5	**138.56**		b				b

[a] See Figure 1 for the structure and atom numbering of **5**. In Figure 6 the 1D ^{13}C NMR spectrum of **5** is shown. Quaternary carbon atoms are typeset in boldface and the multiplicity of the ^1H chemical shifts are indicated between parentheses.

[b] HETCOR cross-peaks are indicated as HT. LR-HETCOR experiments gave the cross-peaks shown as observed with long-range coupling constants of 10 Hz (a) 4 Hz (b) and 10 Hz (c).

135.63 signals. Consequently, these signals can be assigned to C*2*, C*5* and C*18*. Since δ 131.52 and 138.56 belongs to either C*5* or C*18*, the ^{13}C resonance at δ 135.63 has to originate from C*2*. Note that in the 1D ^{13}C NMR spectrum of **5**, the resonance at δ 138.56 is slightly more intense than that at δ 131.52 (Fig. 6). Hence, the resonance at δ 138.56 most likely corresponds to C*5*, since the more distant a carbon atom is from a molecular perimeter, the lower the intensity of the signal will be.[34] This leaves δ 131.52 for C*18*. In addition, the ^{13}C signal at δ 127.96 is more intense than that positioned at δ 120.10; this allows their assignment to C*7* and C*16*, respectively. By elimination, the ^{13}C resonance at δ 114.71 then belongs to C*17*. The complete ^1H and ^{13}C assignments of **5** are summarized in Table 4.

2.2. Computed ^{13}C chemical shifts

In a previous paper,[25] we have tentatively assigned the ^1H NMR resonances of CP-PAHs **1**–**5** using computed ^1H chemical shifts obtained with the *PZ2* (paramagnetic zero) variant[35] of the all electron ab initio continuous transformation of origin of current density (CTOCD) method with the 6-31G** basis as implemented in the Exeter version of SYSMO[36] using 6-31G optimized geometries (see Section 4.2). Although the computed ^1H NMR chemical shifts of **1**–**5** deviate by ca. 0.5 ppm from their experimental values, they satisfactorily reflect the trends found in the experimental ^1H NMR spectra (see also Ref. 23). These observations prompted us to compute the ^{13}C NMR chemical shifts of **1**–**5** using the same CTOCD-*PZ2*/6-31G**//6-31G approach (Table 5 for **3**–**5** and Table 6 for **1**–**2**). For ^{13}C NMR chemical shifts, which span a considerably wider range in parts per

Table 5. CTOCD-*PZ2*/6-31G**//6-31G computed ab initio absolute carbon nuclear shielding constants (σ_{av} in parts per million) of dicyclopenta[*cd*,*fg*]- (**3**), dicyclopenta[*cd*,*jk*]- (**4**) and dicyclopenta[*cd*,*mn*]pyrene (**5**) (see Fig. 1 for a generalized atom numbering scheme)[a]

Compound	Nucleus	σ_{out}	σ_{in}	σ_{av}	δ_{calcd}	δ_{exp}	$\Delta\delta$[b]
3	C*1*	185.3	−1.0	61.1	124.5	123.45	1.05
	C2	160.5	−12.2	45.4	140.2	140.24	−0.04
	C*3*	145.1	−4.3	45.5	140.1	137.31	2.79
	C*4*	153.3	6.8	45.5	130.0	127.88	2.12
	C5	146.1	−3.0	46.7	138.9	137.95	0.95
	C*13*	168.6	2.1	57.6	128.0	127.03	0.97
	C14	192.4	−15.0	54.1	131.5	130.62	0.88
	C*15*	177.4	−1.2	58.3	127.3	127.07	0.23
	C17	197.9	−3.2	63.8	121.8	120.91	0.89
	C18	169.0	−3.0	54.3	131.3	131.23	0.07
4	C*1*	185.2	0.8	62.3	123.3	122.40	0.90
	C2	160.1	−12.7	44.9	140.7	141.00	−0.30
	C*3*	146.5	0.7	49.3	136.3	133.49	2.81
	C*4*	149.4	2.3	51.3	134.2	131.63	2.57
	C5	147.8	−4.5	46.3	139.3	140.42	−1.12
	C*13*	167.0	2.9	57.6	128.0	125.72	2.28
	C14	186.7	−13.7	53.1	132.5	132.07	0.43
	C*15*	176.3	−4.6	55.7	129.9	129.63	0.27
	C17	198.1	−3.6	63.6	122.0	121.45	0.55
	C18	173.4	−2.5	56.2	129.4	130.66	−1.26
5	C*1*	183.3	1.6	62.2	123.4	118.78	4.62
	C2	159.8	−3.5	50.9	134.7	135.63	−0.93
	C*3*	148.6	−5.1	46.1	139.5	135.03	4.47
	C*4*	152.1	9.0	56.7	128.9	126.53	2.37
	C5	158.6	−7.6	47.8	137.8	138.56	−0.76
	C*6*	165.2	2.4	56.6	129.0	125.80	3.20
	C7	191.0	−14.1	54.3	131.3	127.96	3.34
	C*8*	178.5	−11.8	51.6	134.0	132.76	1.24
	C*9*	187.7	−3.7	60.1	125.5	127.04	−1.54
	C16	204.0	−8.8	62.1	123.5	120.10	3.40
	C17	209.1	2.3	71.3	114.3	114.71	−0.41
	C18	178.2	−7.6	47.8	129.8	131.52	−1.72

[a] σ_{out} is the component of the absolute shielding out-of-plane of the ring, σ_{in} is the mean shielding in-plane and σ_{av} the overall mean value. The corresponding δ values (expressed in parts per million) were obtained by the rule $\sigma_{av}\times10^6+\delta=185.6$ (see Section 4.2). [38]Quaternary carbon atoms are typeset in boldface.

[b] $\Delta\delta=\delta_{calcd}-\delta_{exp}$.

Table 6. CTOCD-*PZ2*/6-31G**//6-31G computed ab initio absolute carbon nuclear shielding constants (σ_{av} in parts per million) of pyrene (**1**) and cyclopenta[*cd*]pyrene (**2**, See Fig. 1 for a generalized atom numbering scheme)[a]

Compound	Nucleus	σ_{out}	σ_{in}	σ_{av}	δ_{calcd}	δ_{exp}	$\Delta\delta$[b]
1	C*1*	191.9	−7.5	58.9	126.7	125.78	0.92
	C*2*	177.9	0.8	59.8	125.8	124.87	0.93
	C*5*	167.4	2.7	57.6	128.0	127.32	0.68
	C*17*	200.5	−11.6	59.1	126.5	124.61	1.89
	C*18*	194.6	−16.8	53.7	131.9	131.08	0.82
2	C*1*	186.8	−2.5	60.6	125.0	124.34	0.66
	C2	163.7	−7.3	49.7	135.9	135.58	0.32
	C*3*	149.6	−1.7	48.7	136.9	133.48	3.42
	C*4*	152.9	6.5	55.3	130.3	127.81	2.49
	C5	154.9	−5.8	47.8	137.8	139.07	−1.27
	C*6*	164.3	3.0	56.7	128.9	126.48	2.42
	C*7*	190.9	−15.2	53.5	132.1	131.90	0.20
	C*8*	177.4	−6.9	54.5	131.1	130.52	0.58
	C*9*	189.9	−5.2	59.8	125.8	126.94	−1.14
	C*10*	178.9	−5.0	56.3	129.3	128.54	0.76
	C*11*	195.7	−15.0	55.2	130.4	130.18	0.22
	C*12*	167.9	2.1	57.4	128.2	126.93	1.27
	C*13*	170.6	2.1	58.3	127.3	126.57	0.73
	C*14*	193.4	−16.9	53.2	132.4	130.87	1.53
	C*15*	176.5	3.5	61.1	124.5	122.68	1.82
	C*16*	201.0	−9.3	60.8	124.8	122.23	2.57
	C*17*	203.5	−5.5	64.1	121.5	120.69	0.81
	C*18*	180.2	−4.0	57.4	128.2	127.34	0.86

[a] σ_{out} is the component of the absolute shielding out-of-plane of the ring, σ_{in} is the mean shielding in-plane and σ_{av} the overall mean value. The corresponding δ values (expressed in parts per million) were obtained by the rule $\sigma_{av} \times 10^6 + \delta = 185.6$ (see Section 4.2).[38] Quaternary carbon atoms are typeset in boldface.

[b] $\Delta\delta = \delta_{calcd} - \delta_{exp}$.

million, the deviations between the computed and experimental values, which appear to be the most significant for the carbon atoms of the cyclopenta moieties (range 2.1–4.5 ppm), are still sufficiently small (for all carbon atoms: range 0.0–4.6 ppm, see $\Delta\delta$ values in Tables 5 and 6) to render the computations a material aid for ^{13}C assignments at least in π-conjugated polycyclics. This is to an extent a fortunate consequence of the combination of basis set (6-31G**) and the CTOCD-*PZ2* method, as the results for ^{13}C shifts in the 6-31G** basis can be closer to experiment than 'accurate' Hartree–Fock limiting results.[37]

For **1**–**5** the computed ^{13}C chemical shifts can thus be used to validate the experimental LR-HETCOR ^{13}C assignments (Tables 5 and 6). As shown by the data, the assignments in which the intensity of the ^{13}C signals (cf. compounds **2**, **4** and **5**, vide supra) was used are confirmed by the computed CTOCD-*PZ2*/6-31G**//6-31G ^{13}C chemical shifts.

A comparison of the absolute carbon nuclear shield constants (σ_{av}) of **1**–**5** and their out-of-plane (σ_{out}) and mean in-plane (σ_{in}) components reveal that all carbon sites possess a large diamagnetic, σ_{out} component. The in-plane principal components approximately cancel each other leaving a relatively small, usually paramagnetic, mean in-plane σ_{in} value (Table 5). Similar behaviour has been found for other CP-PAHs.[38]

2.3. Substituent-induced ^{13}C chemical shifts: $\Delta\delta$

To gain insight into the extent to which mono- and dicyclopenta annelation influences the ^{13}C NMR chemical shifts of related carbon positions Substituent-Induced Chemical Shifts (SCS; ^{13}C $\Delta\delta$ in parts per million) were calculated using either the experimental or computed ab initio CTOCD-*PZ2*/6-31G**/6-31G ^{13}C chemical shifts. For the calculation of SCS $\Delta\delta_{exp}$ and $\Delta\delta_{calcd}$ values for CP-PAHs **3**–**5**, the ^{13}C chemical shifts of cyclopenta[*cd*]pyrene (**2**), were taken as a reference ($\Delta\delta_{exp}$(**2**) vs $\Delta\delta_{calcd}$ (**2**), Table 7). The $\Delta\delta_{exp}$ (**2**) and $\Delta\delta_{calcd}$ (**2**) values consistently show that the five-membered ring *ipso* carbon atoms of **3** and **4** behave differently from those of **5** (Table 7). The *ipso* carbon atom C*2* (Fig. 1) of **3** and **4** are deshielded by ca. 4–5 ppm ($\Delta\delta_{exp}$ (**2**) and $\Delta\delta_{calcd}$ (**2**)), whereas the other *ipso* carbon C*5* is

Table 7. Computed CTOCD-*PZ2*/6-31G**//6-31G ab initio ($\Delta\delta_{calcd}$) and experimental ($\Delta\delta_{exp}$) ^{13}C substituent-induced chemical shifts ($\Delta\delta$ (**2**); relative to cyclopenta[*cd*]pyrene (**2**)) for dicyclopenta[*cd*,*fg*]- (**3**), dicyclopenta[*cd*,*jk*]- (**4**) and dicyclopenta[*cd*,*mn*]pyrene (**5**, see Fig. 1 and also Tables 5 and 6)

Nucleus	**3**		**4**		**5**	
	$\Delta\delta$ (**2**)		$\Delta\delta$ (**2**)		$\Delta\delta$ (**2**)	
	Calcd	Exp	Calcd	Exp	Calcd	Exp
C*1*	−0.50	−0.89	−1.70	−1.94	−1.60	−5.57
C2	4.30	4.66	4.80	5.41	−1.20	0.05
C*3*	3.20	3.83	−0.60	0.01	2.60	1.55
C*4*	−0.30	0.06	3.90	3.82	−1.40	−1.28
C5	1.10	−1.13	1.50	1.35	0.00	−0.51
C*6*	**C5**[a]	**C5**[a]	C*13*[a]	C*13*[a]	0.10	−0.69
C*7*	**C*18***[a]	**C*18***[a]	**C*14***[a]	**C*14***[a]	−0.80	−4.34
C*8*	**C2**[a]	**C2**[a]	C*15*[a]	C*15*[a]	2.90	2.24
C*9*	C*1*[a]	C*1*[a]	C*1*[a]	C*1*[a]	−0.30	0.10
C*10*	C*15*[a]	C*15*[a]	**C2**[a]	**C2**[a]	[a]C*8*	[a]C8
C*11*	**C*14***[a]	**C*14***[a]	**C*18***[a]	**C*18***[a]	**C*7***[a]	**C*7***[a]
C*12*	C*13*[a]	C*13*[a]	**C5**[a]	**C5**[a]	C*6*[a]	C*6*[a]
C*13*	0.70	0.46	0.70	−0.85	**C5**[a]	**C5**[a]
C*14*	−0.90	−0.25	0.10	1.20	**C*18***[a]	**C*18***[a]
C*15*	2.80	4.39	5.40	6.95	**C2**[a]	**C2**[a]
C*16*	**C*17***[a]	**C*17***[a]	**C*17***[a]	**C*17***[a]	−1.30	−2.14
C*17*	0.50	0.22	0.30	0.75	−7.20	−5.98
C*18*	1.20	3.89	1.80	3.32	1.60	4.18

[a] Positions equivalent by molecular symmetry; quaternary carbon atoms are typeset in boldface.

slightly shielded in **3** ($\Delta\delta_{exp}$ (**2**), −1.13 ppm) but deshielded in **4** ($\Delta\delta_{exp}$ (**2**), 1.35 ppm). The corresponding $\Delta\delta_{calcd}$ (**2**) values are ca. 1 ppm for C*5* in both **3** and **4**. In contrast, the related $\Delta\delta_{exp}$ (**2**) values for **5** are 0.05 (C*2*) and −0.51 (C*5*) (for comparison: $\Delta\delta_{calcd}$ (**2**), −1.20 (C*2*) and 0.00 (C*5*)). This confirms that the topology of the two annelated cyclopenta moieties affects the electronic structure of **3–5** (see also Ref. 19). This is further substantiated by the $\Delta\delta_{exp}$ (**2**) and $\Delta\delta_{calcd}$ (**2**) values found for some of the more distant carbon atoms (e.g., C*8*, C*10*, C*15*, C*17* and C*18*) in the series **3–5** (Table 7 and Fig. 1), in which all the carbon atoms show a different response.

3. Conclusions

Complete ^{1}H and ^{13}C NMR assignments for the nonalternant (di-) cyclopenta-fused pyrene congeners **3–5** are reported. The experimental assignments are corroborated by chemical shift calculations using the all electron ab initio CTOCD-*PZ2*/6-31G** method. A comparison of the SCS values, $\Delta\delta_{exp}$ (**2**) and $\Delta\delta_{calcd}$ (**2**), shows that for **3–5** with **2** as a reference the number and topology of the annelated cyclopenta moieties markedly affects their electronic structure.

4. Experimental

CP-PAHs **2–5** were synthesized using Flash Vacuum Thermolysis (FVT). The corresponding (1-choroethenyl)-substituted PAH precursors were prepared as described previously.[1–3] Pure CP-PAHs **2–5** were isolated from the pyrolysates by re-crystallization from *n*-hexane. Caution: CP-PAHs **2–5** have to be handled according to the NIH guidelines for carcinogens (see also Ref. 16).

4.1. NMR spectroscopy

^{1}H and ^{13}C NMR spectra were recorded at 25 °C (Varian Unity Inova Spectrometer operating at 300.13 and 75.47 MHz, respectively). The two-dimensional (2D) NMR experiments were also performed on the Varian Unity Inova Spectrometer at 25 °C. In all the experiments, saturated $CDCl_3$ solutions of the CP-PAH **1–5** were used. ^{1}H and ^{13}C NMR chemical shifts are reported in parts per million using residual $CHCl_3$ (δ 7.26 ppm) and $CDCl_3$ (δ 77.00 ppm), respectively, as an internal standard.

Prior to the Long-Range-Heteronuclear Chemical Shift Correlation LR-HETCOR experiments, the proton-coupled C–H ^{13}C spectra of **2–5** were collected to establish the magnitude of $^1J_{C\text{–}H}$ coupling constants. The ^{1}H decay time (T_1) was determined in order to optimise the relaxation delay in the 2D NMR experiments. Nuclear Overhauser Effect Spectroscopy (NOESY): the relaxation delay was set approximately at T_1 for each compound, mixing time 0.75 s, acquisition time 1.3 s, 2D width 700 Hz and number of increments 64. The recording time of the NOESY spectra was in the range 12–20 h. HETCOR and LR-HETCOR: in the HETCOR and LR-HETCOR experiments, a $^1J_{C\text{–}H}$= 160 Hz coupling constant was used. The relaxation delay was set as 1 s for HETCOR and as either 1 s or 4 s for LR-HETCOR in order to obtain the two- ($^2J_{C\text{–}H}$) and three-bond ($^3J_{C\text{–}H}$) C–H coupling constants. HETCOR and LR-HETCOR experiments were recorded with a proton and carbon sweep width of 500–600 and 2500–3000 Hz, respectively. The number of increments was 32. Recording times were ca. 24 h for the HETCOR spectra and 60–72 h for the LR-HETCOR spectra.

4.2. Computations

The absolute carbon nuclear shielding constants (σ_{av} in parts per million), their out-of-plane (σ_{out} in parts per million) and mean in-plane (σ_{in} in parts per million) components of CP-PAH **1–5** were computed using the *PZ2* (paramagnetic zero) variant[38] of the all electron ab initio continuous transformation of origin of current density (CTOCD) method as implemented in the Exeter version of SYSMO,[36] all within the 6-31G** basis. The σ_{av} values (σ_{av}=1/3(σ_{out}+2σ_{in})) were converted into δ values by the rule $\sigma_{av}\times10^6+\delta=185.6$.[37]

The molecular geometries of **1–5** were optimized at the restricted Hartree–Fock level in the 6-31G basis using the GAMESS-UK program[39] and were taken from a previous study.[25] All optimised geometries (**1** (D_{2h}), **2** (C_s), **3** (C_{2v}), **4** (C_{2h}) and **5** (C_{2v})) were characterized as genuine minima by Hessian calculations.

Acknowledgements

Financial support from the Basque Country Government (Eusko Jaurlaritza—Gobierno Vasco, Beca para Formación de Investigadores (M.J.O.-L.)), the Netherlands Organisation for Scientific Research NWO (R.W.A.H., grant 700.53.401) and the Royal Society of Chemistry's Journal Grants for International Authors Programme (0301433, L.W.J.) is gratefully acknowledged.

References and notes

1. Sarobe, M.; Zwikker, J. W.; Snoeijer, J. D.; Wiersum, U. E.; Jenneskens, L. W. *J. Chem. Soc., Chem. Commun.* **1994**, 89–90 and references cited.
2. Sarobe, M.; Flink, S.; Jenneskens, L. W.; van Poecke, B. L. A.; Zwikker, J. W. *J. Chem. Soc., Chem. Commun.* **1995**, 2415–2416.
3. Scott, L. T.; Necula, A. *J. Org. Chem.* **1996**, *61*, 386–388.
4. Lafleur, A. L.; Howard, J. B.; Plummer, E. F.; Taghizadeh, K.; Necula, A.; Scott, L. T.; Swallow, K. C. *Polycyclic Aromat. Compd.* **1998**, *12*, 223–237.
5. Lafleur, A. L.; Howard, J. B.; Taghizadeh, K.; Plummer, E. F.; Scott, L. T.; Necula, A.; Swallow, K. C. *J. Phys. Chem.* **1996**, *100*, 17421–17428.
6. Ledesma, E. B.; Kalish, M. A.; Wornat, M. J.; Nelson, P. F.; Mackie, J. C. *Energy Fuels* **1999**, *13*, 1167–1172.
7. Richter, H.; Risoul, V.; Lafleur, A. L.; Plummer, E. F.; Howard, J. B.; Peters, W. A. *Environ. Health Perspect.* **2000**, *108*, 709–717.
8. Harvey, R. *PAH: Chemistry and Carcinogenicity*; Cambridge University Press: Cambridge, UK, 1991.
9. Fu, P. P.; Beland, F. A.; Yang, S. K. *Carcinogenesis* **1980**, *1*, 725–727.
10. Nesnow, S.; Gold, A.; Mohapatra, N.; Sangaiah, R.; Bryant, B. J.; McNair, P.; Ellis, S. *Genetic Toxicology of Environmental Chemicals, Part A: Basic Principles and Mechanisms of*

Action; Ramel, C., Lambert, B., Magnusson, J., Eds.; Alan R. Liss: New York, NY, 1986; pp 512–515.

11. Sangaiah, R.; Gold, A.; Toney, G. E.; Toney, S. H.; Claxton, L.; Easterling, R.; Nesnow, S. *Mutat. Res.* **1983**, *119*, 259–266.
12. Ball, L. M.; Warren, S. H.; Sangaiah, R.; Gold, A. *Mutat. Res.* **1991**, *260*, 271–279.
13. Ball, L. M.; Warren, S. H.; Sangaiah, R.; Nesnow, S.; Gold, A. *Mutat. Res.* **1989**, *224*, 115–125.
14. Busby, W. F., Jr.; Smith, H.; Plummer, E. F.; Lafleur, A. L.; Mulder, P. P. Y.; Boere, B. B.; Cornelisse, J.; Lugtenburg, J. *Mutat. Res.* **1997**, *391*, 117–125.
15. Lafleur, A. L.; Longwell, J. P.; Marr, J. A.; Monchamp, P. A.; Plummer, E. F.; Thilly, W. G.; Mulder, P. P. Y.; Boere, B. B.; Cornelisse, J.; Lugtenburg, J. *Environ. Health Perspect.* **1993**, *101*, 146–153.
16. Otero-Lobato, M. J.; Jenneskens, L. W.; Seinen, W. *Mutat. Res.* **2004**, *559*, 105–119; Otero-Lobato, M. J.; Kaats-Richters, V. E. M.; Havenith, R. W. A.; Jenneskens, L. W.; Seinen, W. *Mutat. Res.* **2004**, *564*, 39–50; Otero-Lobato, M. J.; Kaats-Richters, V. E. M.; Koper, C.; Vlietstra, E. J.; Havenith, R. W. A.; Jenneskens, L. W.; Seinen, W. *Mutat. Res.* **2005**, *581*, 115–132.
17. Streitwieser, A. *Molecular Orbital Theory for Organic Chemists, Vol. XVI*; Wiley: New York, NY, 1961.
18. Koper, C.; Jenneskens, L. W.; Sarobe, M. *Tetrahedron Lett.* **2002**, *43*, 3833–3836.
19. Koper, C.; Sarobe, M.; Jenneskens, L. W. *Phys. Chem. Chem. Phys.* **2004**, *6*, 319–327.
20. Sarobe, M. Polycyclic Aromatic Hydrocarbons under High Temperature Conditions. Ph. D. Thesis, Consequences for Carbon Build up During Combustion and Fullerene Formation Processes, Utrecht University, Utrecht, The Netherlands, 1998.
21. Sarobe, M.; Snoeijer, J. D.; Jenneskens, L. W.; Slagt, M. Q.; Zwikker, J. W. *Tetrahedron Lett.* **1995**, *36*, 8489–8492.
22. Gooijer, C.; Kozin, I.; Velthorst, N. H.; Sarobe, M.; Jenneskens, L. W.; Vlietstra, E. J. *Spectrochim. Acta, Part A* **1998**, *54*, 1443–1449.
23. Havenith, R. W. A.; Jiao, H.; Jenneskens, L. W.; van Lenthe, J. H.; Schleyer, P. v. R.; Kataoka, M.; Necula, A.; Scott, L. T. *J. Am. Chem. Soc.* **2002**, *124*, 2363–2370.
24. Havenith, R. W. A.; van Lenthe, J. H.; Dijkstra, F.; Jenneskens, L. W. *J. Phys. Chem. A* **2001**, *105*, 3838–3845.
25. Steiner, E.; Fowler, P. W.; Jenneskens, L. W.; Havenith, R. W. A. *Eur. J. Org. Chem.* **2002**, 163–169.
26. Homann, K.-H. *Angew. Chem., Int. Ed.* **1998**, *37*, 2434–2451.
27. Taylor, R.; Langley, G. J.; Kroto, H. W.; Walton, D. R. M. *Nature* **1993**, *366*, 728–731.
28. Rabideau, P. W.; Sygula, A. *Acc. Chem. Res.* **1996**, *29*, 235–242.
29. Jans, A. W. H.; Tintel, C.; Cornelisse, J.; Lugtenburg, J. *Magn. Reson. Chem.* **1986**, *24*, 101–104.
30. Dosa, P. I.; Schleifenbaum, A.; Vollhardt, K. P. C. *Org. Lett.* **2001**, *3*, 1017–1020.
31. Chang, C.-H.; Floss, H. G.; Steck, W. *J. Org. Chem.* **1977**, *42*, 1337–1340.
32. Sahali, Y.; Kwon, H.; Skipper, P. L.; Tannenbaum, S. R. *Chem. Res. Toxicol.* **1992**, *5*, 157–162.
33. Claridge, T. D. W. *High-Resolution NMR Techniques in Organic Chemistry*; Pergamon: New York, NY, 1999; pp 221–257.
34. Kalinowski, H. O.; Berger, S.; Braun, S. *^{13}C NMR Spektroskopie*; Thieme: Stuttgart, 1984; Chapter 5.
35. Zanasi, R.; Lazzeretti, P.; Malagoli, M.; Piccinini, F. *J. Chem. Phys.* **1995**, *102*, 7150–7157.
36. Lazzeretti, P.; Zanasi, R. *SYSMO Package*; University of Modena, 1980.
37. Zanasi, R. *J. Chem. Phys.* **1996**, *105*, 1460–1469.
38. Fowler, P. W.; Steiner, E.; Acocella, A.; Jenneskens, L. W.; Havenith, R. W. A. *J. Chem. Soc., Perkin Trans. 2* **2001**, 1058–1065.
39. Guest, M. F.; Bush, I. J.; van Dam, H. J. J.; Sherwood, P.; Thomas, J. M. H.; van Lenthe, J. H.; Havenith, R. W. A.; Kendrick, J. *Mol. Phys.* **2005**, *103*, 719–747.